PERGAMON

International Journal of Solids and Structures 38 (2001) 2769–2788

INTERNATIONAL JOURNAL OF SOLIDS and STRUCTURES

www.elsevier.com/locate/ijsolstr

Thermal shock stresses due to heat convection at a bounding surface in a thick orthotropic cylindrical shell

H. Cho [a], G.A. Kardomateas [b,*]

[a] *Department of Aerospace Engineering, Air Force Academy, Cheongju, South Korea*
[b] *School of Aerospace Engineering, Georgia Institute of Technology, Atlanta, GA 30332-0150, USA*

Received 21 January 1999; in revised form 4 February 2000

Abstract

A closed form elastodynamic solution for the thermal shock stresses due to heat transfer into/from a medium (e.g. fluid) at a constant temperature in a thick orthotropic cylindrical shell is developed. Temperature distribution varies with time and space throughout the shell thickness. The mathematical formulation is done by the three-dimensional linear dynamic elasticity approach and the use of appropriate integral transforms such as the finite Hankel transform and the Laplace transform. No restrictions are imposed regarding the shell thickness in the formulation. The present case, which is more practical and general, is an extension of the case of uniform heating previously studied by the authors. Numerical results show the role of the stress wave propagation and reflection in conjunction with the thermal and material orthotropy. These have a significant influence on the dynamic thermal shock stresses through the shell thickness. Results present the complete dynamic response of thermal shock stresses using realistic inertia parameters and material properties in a thick orthotropic cylindrical shell made out of glass/epoxy.

Keywords: Thermal stresses; Shell; Orthotropic; Elastodynamic

1. Introduction

The thermally excited mechanical response of cylindrical shell composite structures is of interest in various applications of spacecraft, space station, aircraft, ship, submarine and nuclear plant technology as well as chemical pipes. These structures can be exposed to thermal environments with a rapidly changing temperature. Information for the thermal stress analysis is necessary in the safe design of these types of structural applications. In the case of rapidly changing temperature, dynamic thermoelasticity should be considered, since the inertia would play a nonnegligible role on the thermal deformations which would result in these elastic bodies.

Dynamic thermoelastic problems have been studied, since several decades, in infinite or semi-infinite elastic bodies and in hollow spherical shells. In particular, thermal shock stresses in an elastic infinite

* Corresponding author. Tel.: +1-404-894-8198; fax: +1-404-894-2760.
E-mail address: gkardoma@mail.ae.gatech.edu (G.A. Kardomateas).

0020-7683/01/$ - see front matter
PII: S0020-7683(00)00181-5

medium with a spherical cavity were studied by Sternberg and Chakravorty (1959) by the method of Laplace transforms. Later, the same method of Laplace transforms was applied to the thermal stress wave propagation problem under rapid loading in hollow spheres by Tsui and Kraus (1965). Another early work by Zaker (1969) presented a linear dynamic thermoelasticity study for the thermal shock stresses using the method of image. These studies included the heat conduction equation for the transient temperature distribution. These early works provide useful fundamental insights and understanding of the distribution of thermal shock stresses and the stress wave propagation through the wall of structures. Hata (1991) applied the Ray theory to the thermal shock problem using the decomposed displacement potentials in a hollow sphere under rapid uniform heating without considering the transient temperature distribution. Recently, Wang (1995) studied the thermal shock stress problem in an isotropic hollow cylinder by using integral transforms such as the finite Hankel transform and the Laplace transform. Such applications of the finite Hankel transform and the Laplace transform to boundary value problems in a hollow cylinder were originally developed by Cinelli (1965).

As far as static thermal stress analyses by the elasticity approach for orthotropic cylindrical shells, a solution was presented by Kardomateas (1989, 1990) for the transient thermal stresses in a filament wound orthotropic thick cylindrical shell. Similar works without the transient temperature were presented by Hyer and Cooper (1986) for circumferentially varying loading and by Yuan (1993) using potential functions. Although these researchers have studied this configuration, the investigations are mostly confined to the static analysis, i.e., the inertia term is not considered. On the contrary, Cho et al. (1998) included the inertia term and studied the elastodynamic thermal shock stresses due to uniform heating in a thick orthotropic cylindrical shell using integral transforms. Also, a numerical solution in plain strain condition is reported by Sumi and Ito (1993) for thermal shock stresses in orthotropic cylindrical or spherical shells using the finite difference method. In their work, numerical examples were presented using an inertia parameter which does not seem, however, to represent typical materials. The inertia parameter is important because it determines the wave propagation time in the wall.

In general, limited investigations of thermoelastic waves through the thickness of composite cylindrical shells exist, even though several linear dynamic thermoelastic problems have been studied for isotropy. In particular, there have not been any elastodynamic closed form solutions yet reported for thermal shock stresses in orthotropic thick cylindrical shells considering the transient temperature through the thickness. This work, which extends the previous work of the authors (Cho et al., 1998), presents a three-dimensional elastodynamic solution for the thermal shock stresses in the wall of an orthotropic thick cylindrical shell. The transient temperature distribution can occur due to heat conduction through the shell thickness. The loading circumstance of a constant temperature suddenly applied at one surface boundary and spreading over the thickness can be easily seen in many industrial applications. The proper usage of integral transforms such as the finite Hankel transform and the Laplace transform for the dynamic part of the governing equations leads to a closed form elastodynamic solution.

2. Formulation

Consider a hollow cylinder subjected to a temperature distribution with or without external pressure. The inner and outer radii are denoted by r_1 and r_2, respectively. We denote by r, the radial, θ, the circumferential, and z, the axial coordinate. The hollow cylinder is assumed to have zero initial temperature. The temperature distribution is obtained by solving the heat conduction equation given by

$$\frac{\partial T(r,t)}{\partial t} = K\left[\frac{\partial^2 T(r,t)}{\partial r^2} + \frac{1}{r}\frac{\partial T(r,t)}{\partial r}\right], \quad (r_1 \leqslant r \leqslant r_2,\ t > 0), \tag{1}$$

where K is the thermal diffusivity of the composite in the r direction.

The initial and general boundary conditions are

$$T(r,0) = 0 \quad \text{at } r_1 \leqslant r \leqslant r_2, \tag{2a}$$

$$h_1 \frac{\partial T(r,t)}{\partial t}\Big|_{r=r_1} - h_2 T(r_1,t) = h_3 \quad (t>0), \tag{2b}$$

$$h_1^* \frac{\partial T(r,t)}{\partial t}\Big|_{r=r_2} + h_2^* T(r_2,t) = h_3^* \quad (t>0), \tag{2c}$$

where h_1, h_2, h_1^* and h_2^* are constants which may be positive or zero and h_3 and h_3^* are also constants. By choice of these constants, the general results include all combinations of constant temperature, constant heat flux, zero heat flux, or heat convection to a different medium at either surface. The distribution of temperature $T(r,t)$ in the wall is given by Carslaw and Jaeger (1959) for the hollow cylinder in terms of the Bessel functions of the first and second kind $J_n(x)$ and $Y_n(x)$, as follows:

$$T(r,t) = d_1 + d_2 \ln(r_2/r) + d_3 \ln(r/r_1) + \sum_{n=1}^{\infty} \mathrm{e}^{-K\alpha_n{}^2 t}[d_{4n} J_0(r\alpha_n) + d_{5n} Y_0(r\alpha_n)], \tag{3}$$

where d_1, d_2, d_3, d_{4n} and d_{5n} are constants (d_{4n} and d_{5n} are shown in Appendix A). Also, α_n are the positive roots of the following transcendental equation:

$$[h_1\alpha J_1(r_1\alpha) + h_2 J_0(r_1\alpha)]\left[h_1^*\alpha Y_1(r_2\alpha) - h_2^* Y_0(r_2\alpha)\right] - [h_1 Y_1(r_1\alpha) + h_2 Y_0(r_1\alpha)] \times \left[h_1^*\alpha J_1(r_2\alpha) - h_2^* J_0(r_2)\right] = 0. \tag{4}$$

Since there is only radial dependence of the temperature field (3), the hoop displacements are zero and the stresses and strains are independent of θ. Thus, the thermoelastic stress–strain relations for the orthotropic body are

$$\begin{bmatrix} \sigma_{rr} \\ \sigma_{\theta\theta} \\ \sigma_{zz} \\ \tau_{\theta z} \\ \tau_{rz} \\ \tau_{r\theta} \end{bmatrix} = \begin{bmatrix} c_{11} & c_{12} & c_{13} & 0 & 0 & 0 \\ c_{12} & c_{22} & c_{23} & 0 & 0 & 0 \\ c_{13} & c_{23} & c_{33} & 0 & 0 & 0 \\ 0 & 0 & 0 & c_{44} & 0 & 0 \\ 0 & 0 & 0 & 0 & c_{55} & 0 \\ 0 & 0 & 0 & 0 & 0 & c_{66} \end{bmatrix} \begin{bmatrix} \epsilon_{rr} - \alpha_r \Delta T \\ \epsilon_{\theta\theta} - \alpha_\theta \Delta T \\ \epsilon_{zz} - \alpha_z \Delta T \\ \gamma_{\theta z} \\ \gamma_{rz} \\ \gamma_{r\theta} \end{bmatrix}, \tag{5}$$

where c_{ij} are the elastic constants and α_i are the thermal expansion coefficients (1, 2, and 3 represent r, θ, and z, respectively.) The geometry of the shell is assumed to be axisymmetric. Since the temperature does not depend on the axial coordinate, it is assumed that the stresses are independent of z. In addition to the constitutive equations (5), the elastic response of the hollow cylinder must satisfy the equilibrium equations. Only one equilibrium elastodynamic equation remains, since $\tau_{\theta z} = \tau_{rz} = \tau_{r\theta} = 0$.

$$\frac{\partial \sigma_{rr}}{\partial r} + \frac{\sigma_{rr} - \sigma_{\theta\theta}}{r} = \rho_{\mathrm{o}} \frac{\partial^2 u_r(r,\theta,z,t)}{\partial t^2}. \tag{6}$$

For the problem without the thermal effects, the following expressions for the displacement field were derived by Lekhnitskii (1981).

$$u_r = U(r,t) + z(w_y \cos\theta - w_x \sin\theta) + u_0 \cos\theta + v_0 \sin\theta, \tag{7a}$$

$$u_\theta = -z(w_y \sin\theta + w_x \cos\theta) + w_z r - u_0 \sin\theta + v_0 \cos\theta, \tag{7b}$$

$$u_z = zf(t) - r(w_y \cos\theta - w_x \sin\theta) + w_0, \tag{7c}$$

where the function $U(r,t)$ represents the radial displacement accompanied by deformation. The constants u_0, v_0, w_0, w_x, w_y, and w_z denote the rigid body translation and rotation along the x, y, and z directions in the Cartesian coordinate system, respectively. The time-dependent parameter $f(t)$ is obtained from boundary conditions.

The strains are expressed in terms of the displacements as follows:

$$\epsilon_{rr} = \frac{\partial U(r,t)}{\partial r}, \qquad \epsilon_{\theta\theta} = \frac{U(r,t)}{r}, \qquad \epsilon_{zz} = f(t), \tag{8a}$$

$$\gamma_{\theta z} = \gamma_{rz} = \gamma_{r\theta} = 0. \tag{8b}$$

Substituting Eqs. (5) and (8) into the equilibrium equation (6), gives the following equation of thermal elastodynamics for the displacement $U(r,t)$:

$$c_{11}\left[\frac{\partial^2 U(r,t)}{\partial r^2} + \frac{1}{r}\frac{\partial U(r,t)}{\partial r}\right] - \frac{c_{22}}{r^2}U(r,t) = q_1\frac{\partial T(r,t)}{\partial r} + q_2\frac{T(r,t)}{r} + (c_{23} - c_{13})\frac{f(t)}{r} + \rho_o\frac{\partial^2 U(r,t)}{\partial t^2}, \tag{9}$$

where the constants q_1 and q_2 are

$$q_1 = c_{11}\alpha_r + c_{12}\alpha_\theta + c_{13}\alpha_z, \tag{10a}$$

$$q_2 = (c_{11} - c_{12})\alpha_r + (c_{12} - c_{22})\alpha_\theta + (c_{13} - c_{23})\alpha_z, \tag{10b}$$

and the initial conditions and the boundary conditions from external tractions $\sigma_{rr}(r_i,t) = \phi_i(t)$ at $r_i = r_1, r_2$ are

$$U(r,0) = 0, \quad \frac{\partial U(r,0)}{\partial t} = 0, \tag{11a}$$

$$c_{11}\frac{\partial U(r_i,t)}{\partial r} + c_{12}\frac{U(r_i,t)}{r} + c_{13}f(t) - q_1 T(r_i,t) = \phi_i(t). \tag{11b}$$

The axial force $P_z(t)$ is given by

$$P_z(t) = \int_{r_1}^{r_2} \sigma_{zz}(r,t)2\pi r\,\mathrm{d}r, \tag{12}$$

or, by using Eqs. (5) and (8)

$$P_z(t) = \int_{r_1}^{r_2}\left[c_{31}\frac{\partial U(r,t)}{\partial r} + c_{32}\frac{U(r,t)}{r} + c_{33}f(t) - q_3 T(r_i,t)\right]2\pi r\,\mathrm{d}r, \tag{13}$$

where $q_3 = c_{31}\alpha_r + c_{32}\alpha_\theta + c_{33}\alpha_z$.

Consider first the quasi-static thermoelastic equation given as follows:

$$c_{11}\left[\frac{\partial^2 U_{st}(r,t)}{\partial r^2} + \frac{1}{r}\frac{\partial U_{st}(r,t)}{\partial r}\right] - \frac{c_{22}}{r^2}U_{st}(r,t) = q_1\frac{\partial T(r,t)}{\partial r} + q_2\frac{T(r,t)}{r} + (c_{23} - c_{13})\frac{f(t)}{r}. \tag{14}$$

Notice that the absence of the inertia term (the last term in Eq. (9)). The associated initial and boundary conditions are given as in Eqs. (11)–(13) with U_{st} substituted in place of U.

Assume that the quasi-static thermoelastic radial displacement can be decomposed into a steady and a transient part as

$$U_{st}(r,t) = U_o(r) + \sum_{n=1}^{\infty} R_n(r)\Omega_n(t), \tag{15}$$

where $\Omega_n(t) = e^{-K\alpha_n^2 t}$ for convenience, and set $f(t)$ in the form

$$f(t) = f_o + \sum_{n=1}^{\infty} f_n\, \Omega_n(t). \tag{16}$$

Expression (15), if it is substituted into Eq. (14), gives the following two inhomogeneous ordinary differential equations of second order for the displacements $U_o(r)$ and $R_n(r)$:

$$c_{11}\left[\frac{\partial^2 U_o(r)}{\partial r^2} + \frac{1}{r}\frac{\partial U_o(r)}{\partial r}\right] - \frac{c_{22}}{r^2}U_o(r) = \frac{q_1(d_3-d_2) + q_2 d_1 + (c_{23}-c_{13})f_o}{r} + q_2 d_2 \frac{\ln(r_2/r)}{r} + q_2 d_3 \times \frac{\ln(r/r_1)}{r}, \tag{17}$$

and for $n = 1, \ldots, \infty$,

$$c_{11}\left[\frac{\partial^2 R_n(r)}{\partial r^2} + \frac{1}{r}\frac{\partial R_n(r)}{\partial r}\right] - \frac{c_{22}}{r^2}R_n(r) = (c_{23}-c_{13})\frac{f_n}{r} + d_{4n}\left[q_2\frac{J_0(r\alpha_n)}{r} - q_1\alpha_n J_1(r\alpha_n)\right] + d_{5n}\left[q_2\frac{Y_0(r\alpha_n)}{r} - q_1\alpha_n Y_1(r\alpha_n)\right]. \tag{18}$$

In this transient thermoelasticity problem, the displacement field was obtained by Kardomateas (1989, 1990). Specifically, the solution $U_o(r)$ of the inhomogeneous differential equation (17) is given by

$$U_o(r) = G_{10}r^{\lambda_1} + G_{20}r^{\lambda_2} + \frac{c_{23}-c_{13}}{c_{11}-c_{22}}f_0 r + U_o^*(r), \tag{19}$$

where

$$U_o^*(r) = \frac{1}{c_{11}-c_{22}}[d_o r + q_2 d_2 r\ln(r_2/r) + q_2 d_3 r\ln(r/r_1)]. \tag{20}$$

Also, $\lambda_{1,2} = \sqrt{c_{22}/c_{11}}$ and the constant d_o is

$$d_o = q_1(d_3-d_2) + q_2 d_1 - \frac{2c_{11}q_2(d_3-d_2)}{(c_{11}-c_{22})}.$$

The solution $R_n(r)$ of the inhomogeneous differential equation (18) is expressed as

$$R_n(r) = G_{1n}r^{\lambda_1} + G_{2n}r^{\lambda_2} + \frac{c_{23}-c_{13}}{c_{11}-c_{22}}f_n r + R_n^*(r), \tag{21}$$

where

$$R_n^*(r) = B_{0n}r + \frac{2q_2 d_{5n}}{\pi(c_{11}-c_{22})}r\ln(r\alpha_n/2) + \sum_{k=0}^{\infty} B_{1nk}r^{2k+3}\ln(r\alpha_n/2) + B_{2nk}r^{2k+3}, \tag{22}$$

with B_{0n} defined as

$$B_{0n} = \frac{d_{4n}q_2 + d_{5n}(2/\pi)(q_1+\gamma q_2)}{(c_{11}-c_{22})} - \frac{4c_{11}q_2 d_{5n}}{\pi(c_{11}-c_{22})}, \tag{23}$$

and B_{1nk} and B_{2nk} provided in Appendix B.

The definition of series expansion for the Bessel functions cannot be used for large arguments. Hence, the particular solution of Eq. (18) for large arguments is needed. This solution can be achieved by using the Hankel asymptotic expansions of the Bessel function of the first and second kind of arbitrary order v. Employing the following substitutions:

$$\rho = r\alpha_n, \quad R_n^{**}(\rho) = R_n^*(r), \tag{24}$$

the equation for $n = 1, \ldots, \infty$ can be expressed by using the asymptotic definitions of the Bessel functions as following:

$$c_{11}\alpha_n^2\left[\frac{\partial^2 R_n(r)}{\partial r^2} + \frac{1}{r}\frac{\partial R_n(r)}{\partial r}\right] - \alpha_n^2\frac{c_{22}}{r^2}R_n(r) = \sum_{k=0}^{\infty}\frac{(-1)^k\alpha_n\psi_1(k)}{(2k)!(8\rho)^{2k}\rho\sqrt{\rho\pi}}\big[(d_{4n}+d_{5n}) \times (q_2\sin\rho - a_{1,k}\rho\cos\rho + a_{2,k}\rho^2\sin\rho) + (d_{4n}-d_{5n}) \times (q_2\cos\rho - a_{1,k}\rho\sin\rho + a_{2,k}\rho^2\cos\rho)\big], \tag{25}$$

where

$$a_{1,k} = q_1\frac{4k+1}{4k-1} - q_2\frac{16k}{(4k-1)^2}, \qquad a_{2,k} = \frac{16kq_1}{(4k-1)(4k-3)}, \tag{26}$$

and $\psi_1(k)$ is defined as follows:

$$\psi_1(k) = 1^2\cdot 3^2\cdot 5^2\cdots(4k-1)^2, \quad k = 1, \infty. \tag{27}$$

The solution to this equation is obtained as

$$R_n^{**}(\rho) = \sum_{k=0}^{\infty} p_{k,1}^n\rho^{-2k-1/2}\cos\rho + s_{k,1}^n\rho^{-2k-1/2}\sin\rho + p_{k,2}^n\rho^{-2k-3/2}\cos\rho + s_{k,2}^n\rho^{-2k-3/2}\sin\rho. \tag{28}$$

The coefficients $p_{k,1}^n$, $s_{k,1}^n$, $p_{k,2}^n$ and $s_{k,2}^n$ are determined from recursive formulas as in (Kardomateas, 1990) by considering the terms in the sum that contribute to the terms $\rho^{-2k-1/2}\cos\rho$, $\rho^{-2k-1/2}\sin\rho$, $\rho^{-2k-3/2}\cos\rho$ and $\rho^{-2k-3/2}\rho\sin\rho$ on the right-hand side of Eq. (25). Solution (28) is a particular solution of Eq. (25) derived by considering the Hankel asymptotic expansions of the Bessel functions for values of the arguments $\rho = r\alpha_n \geqslant \rho_{tr} = 18.0$, i.e. the Hankel asymptotic expansions domain, whereas the solution $R_n^*(r)$, which will be denoted by $R_{nS}^*(r)$, had been derived based on series expansions for the Bessel functions, for values of the argument $\rho \leqslant \rho_{tr}$, i.e. the Bessel functions domain. Since for a given root α_n, the argument ρ ranges from $r_1\alpha_n$ to $r_2\alpha_n$, there may be a transition point from one solution to the other for $R_n^*(r)$ in expression (21). Both solutions are particular ones but may be different. Thus, at that transition point, a homogeneous solution term should be added to Eq. (28) so that

$$R_{nL}^{**}(\rho) = h_{1n}\rho^{\lambda_1} + h_{2n}\rho^{\lambda_2} + R_n^{**}(\rho), \tag{29}$$

where h_{1n} and h_{2n} are determined from the condition of equal value and slope at the transition point:

$$R_{nL}^{**}(\rho) = R_{nS}^*(\rho_{tr}/\alpha_n), \qquad R_{nL}^{**\prime}(\rho) = R_{nS}^{*\prime}(\rho_{tr}/\alpha_n). \tag{30}$$

Now, turning to the total displacement for the linear dynamic thermoelasticity, the general solution of the governing equation (9) is

$$U(r,t) = U_{\mathrm{st}}(r,t) + U_{\mathrm{d}}(r,t), \tag{31}$$

where $U_{\mathrm{st}}(r,t)$ represents the quasi-static thermoelastic radial displacement and $U_{\mathrm{d}}(r,t)$ denotes the dynamic radial displacement. Using Eq. (9) with associated initial and boundary conditions and the above definition, the following elastodynamic equation in terms of the displacement is obtained:

$$c_{11}\left[\frac{\partial^2 U_{\mathrm{d}}(r,t)}{\partial r^2}+\frac{1}{r}\frac{\partial U_{\mathrm{d}}(r,t)}{\partial r}\right]-\frac{c_{22}}{r^2}U_{\mathrm{d}}(r,t)=\rho_{\mathrm{o}}\left[\frac{\partial^2 U_{\mathrm{st}}(r,t)}{\partial t^2}+\frac{\partial^2 U_{\mathrm{d}}(r,t)}{\partial t^2}\right] \tag{32}$$

with the initial conditions

$$U_{\mathrm{d}}(r,0)=0,\qquad \frac{\partial U_{\mathrm{d}}(r,0)}{\partial t}=0, \tag{33}$$

and the boundary conditions of traction-free surfaces of the hollow cylinder

$$c_{11}\frac{\partial U_{\mathrm{d}}(r_i,t)}{\partial r}+c_{12}\frac{U_{\mathrm{d}}(r_i,t)}{r_i}=0,\quad i=1,2, \tag{34}$$

as well as the condition of no axial force at the ends

$$0=\int_{r_1}^{r_2}\left[c_{31}\frac{\partial U_{\mathrm{d}}(r,t)}{\partial r}+c_{32}\frac{U_{\mathrm{d}}(r,t)}{r_i}\right]2\pi r\,\mathrm{d}r. \tag{35}$$

Rewriting the equation of dynamic elasticity (32),

$$\frac{\partial^2 U_{\mathrm{d}}(r,t)}{\partial r^2}+\frac{1}{r}\frac{\partial U_{\mathrm{d}}(r,t)}{\partial r}-\frac{v^2}{r^2}U_{\mathrm{d}}(r,t)=\frac{1}{\bar{c}^2}\left[\frac{\partial^2 U_{\mathrm{st}}(r,t)}{\partial t^2}+\frac{\partial^2 U_{\mathrm{d}}(r,t)}{\partial t^2}\right], \tag{36}$$

where $v=\sqrt{c_{22}/c_{11}}$. Therefore, $v=\lambda_1$ and also the wave speed through the thickness in the cylindrical shell is defined as $\bar{c}=\sqrt{c_{11}/\rho_{\mathrm{o}}}$.

From now on, the procedure for solving the dynamic elasticity equation (36) is needed. The general solution after setting $U_{\mathrm{st}}=0$, is obtained by

$$U_{\mathrm{d}}(r,t)=A(t)J_v(\xi r)+B(t)Y_v(\xi r), \tag{37}$$

where the Bessel function of the second kind of order v is defined as

$$Y_v(\xi r)=\frac{J_v(\xi r)\cos v\pi-J_{-v}(\xi r)}{\sin \pi v}. \tag{38}$$

Notice that when the order v is an integer n, $Y_n=\lim_{v\to n}Y_v(\xi r)$. By using the boundary conditions (34), $U_{\mathrm{d}}(r,t)$ can be written in the eigenfunction series

$$U_{\mathrm{d}}(r,t)=\sum_i A_i(t)D_v(\xi_i r),\quad i=1,2,\ldots,\infty, \tag{39}$$

where the eigenfunctions are in the form

$$D_v(\xi_i r)=J_v(\xi_i r)Y_a-Y_v(\xi_i r)J_a. \tag{40}$$

If $v=n$, the eigenfunctions are in the form

$$D_n(\xi_i r)=J_n(\xi_i r)Y_a-Y_n(\xi_i r)J_a. \tag{41}$$

In these formulas, ξ_i are the positive roots of the transcendental equation

$$J_aY_b-J_bY_a=0, \tag{42}$$

where

$$J_a=\xi_i J_v'(\xi_i r_1)+h_1J_v(\xi_i r_1),\qquad J_b=\xi_i J_v'(\xi_i r_2)+h_2J_v(\xi_i r_2), \tag{43a}$$

$$Y_a=\xi_i Y_v'(\xi_i r_1)+h_1Y_v(\xi_i r_1),\qquad Y_b=\xi_i Y_v'(\xi_i r_2)+h_2Y_v(\xi_i r_2) \tag{43b}$$

and the constants h_i are defined by

$$h_1 = \frac{c_{12}}{r_1 c_{11}}, \qquad h_2 = \frac{c_{12}}{r_2 c_{11}}. \tag{44}$$

In the finite range of the elastic body, $A_i(t)$ can be obtained as

$$A_i(t) = \frac{\int_{r1}^{r2} r U_{\mathrm{d}}(r,t) D_v(\xi_i r)\,\mathrm{d}r}{\int_{r1}^{r2} r[D_v(\xi_i r)]^2\,\mathrm{d}r}. \tag{45}$$

The finite Hankel transform for the dynamic displacement (39) can be written as:

$$\widehat{u_{\mathrm{d}}}(\xi_i,t) = \int_{r_1}^{r_2} r U_{\mathrm{d}}(r,t) D_v(\xi_i r)\,\mathrm{d}r. \tag{46}$$

Then, the inverse of the finite Hankel transform is obtained as

$$U_{\mathrm{d}}(r,t) = \sum_i \frac{\widehat{u_{\mathrm{d}}}(\xi_i,t) D_v(\xi_i r)}{N(\xi_i)}, \tag{47}$$

where $N(\xi_i) = \int_{r1}^{r2} r[D_v(\xi_i r)]^2\,\mathrm{d}r$, is a normalizing factor and is always positive. By the definition of the finite Hankel transform, the transformation of Eq. (32) is given as

$$\begin{aligned}&\frac{2J_a}{\pi J_b}\left[\frac{\partial U_{\mathrm{d}}(r_2,t)}{\partial r} + h_2\frac{U_{\mathrm{d}}(r_2,t)}{r}\right] - \frac{2}{\pi}\left[\frac{\partial U_{\mathrm{d}}(r_1,t)}{\partial r} + h_1\frac{U_{\mathrm{d}}(r_1,t)}{r}\right] - \xi_i^2\widehat{u_{\mathrm{d}}}(\xi_i,t)\\ &\quad = \frac{1}{\bar{c}^2}\left[\frac{\partial^2\widehat{u_{\mathrm{d}}}(\xi_i,t)}{\partial t^2} + \frac{\partial^2\widehat{u_{\mathrm{st}}}(\xi_i,t)}{\partial t^2}\right].\end{aligned} \tag{48}$$

Since $U_{\mathrm{d}}(r,t)$ satisfies the homogeneous boundary conditions (34) at each surface, the first two terms of the left-hand side of Eq. (48) should vanish. Thus, the transformed equation becomes

$$-\xi_i^2\widehat{u_{\mathrm{d}}}(\xi_i,t) = \frac{1}{\bar{c}^2}\left[\frac{\partial^2\widehat{u_{\mathrm{d}}}(\xi_i,t)}{\partial t^2} + \frac{\partial^2\widehat{u_{\mathrm{st}}}(\xi_i,t)}{\partial t^2}\right]. \tag{49}$$

Using the Laplace transform, denoted by $\widehat{u_{\mathrm{d}}}^{\mathrm{L}}$, with the zero initial conditions, the above equation becomes

$$\widehat{u_{\mathrm{d}}}^{\mathrm{L}}(\xi_i,s) = -\widehat{u_{\mathrm{st}}}^{\mathrm{L}}(\xi_i,s) + \frac{\bar{c}^2\xi_i^2}{\bar{c}^2\xi_i^2 + s^2}\widehat{u_{\mathrm{st}}}^{\mathrm{L}}(\xi_i,s), \tag{50}$$

and subsequently, using the inverse Laplace transform, we obtain the following expression:

$$\widehat{u_{\mathrm{d}}}(\xi_i,t) = -\widehat{u_{\mathrm{st}}}(\xi_i,t) + \bar{c}\xi_i \sin\bar{c}\xi_i t * \ \widehat{u_{\mathrm{st}}}(\xi_i,t). \tag{51}$$

Since $U_{\mathrm{st}}(r_i,t)$ is already known, the finite Hankel transform of $U_{\mathrm{st}}(r_i,t)$, denoted by $\widehat{u_{\mathrm{st}}}(\xi_i,t)$, is defined as

$$\widehat{u_{\mathrm{st}}}(\xi_i,t) = \int_{r_1}^{r_2} r U_{\mathrm{st}}(r,t) D_v(\xi_i r)\,\mathrm{d}r. \tag{52}$$

Then, the finite Hankel transform of the thermally induced displacement is

$$\widehat{u_{\mathrm{st}}}(\xi_i,t) = \widehat{U}_{\mathrm{o}}(\xi_i) + \sum_{n=1}^{\infty}\widehat{R}_n(\xi_i)\Omega_n(t), \tag{53}$$

where, by definition, the finite Hankel transforms of $U_{\mathrm{o}}(r)$ and $R_n(r)$ are

$$\widehat{U}_o(\xi_i) = G_{10}I_1(\xi_i) + G_{20}I_2(\xi_i) + f_o\frac{c_{23}-c_{13}}{c_{11}-c_{22}}I_3(\xi_i) + d_oI_3(\xi_i) + \frac{q_2d_2}{c_{11}-c_{22}}I_4(\xi_i) + \frac{q_2d_3}{c_{11}-c_{22}}I_5(\xi_i). \tag{54}$$

For $n = 1, \infty$,

$$\widehat{R}_n(\xi_i) = G_{1n}I_1(\xi_i) + G_{2n}I_2(\xi_i) + f_n\frac{c_{23}-c_{13}}{c_{11}-c_{22}}I_3(\xi_i) + B_{0n}I_3(\xi_i) + B'_{0n}I_6(\xi_i) + \sum_{k=0}^{\infty} B_{1nk}I_7(\xi_i) + B_{2nk}I_8(\xi_i), \tag{55}$$

In the large argument range, the finite Hankel transform should be evaluated by using solution (28) and (29), then

$$\widehat{R}_n(\xi_i) = (G_{1n} + \alpha_n^{\lambda_1}d_{6n})I_1(\xi_i) + (G_{2n} + \alpha_n^{\lambda_2}d_{7n})I_2(\xi_i) + f_n\frac{c_{23}-c_{13}}{c_{11}-c_{22}}I_3(\xi_i) + \sum_{k=0}^{\infty} p^n_{k,1}I_{6L}(\xi_i) + s^n_{k,1}I_{7L}(\xi_i) + p^n_{k,2}I_{8L}(\xi_i) + s^n_{k,2}I_{9L}(\xi_i). \tag{56}$$

In order to evaluate the above integral transforms the following integrals are needed:

$$I_1(\xi_i) = \int_{r_1}^{r_2} r^{v+1}D_v(\xi_i r)\,\mathrm{d}r, \qquad I_2(\xi_i) = \int_{r_1}^{r_2} r^{-v+1}D_v(\xi_i r)\,\mathrm{d}r. \tag{57}$$

From the recurrence formulas $\mathrm{d}[z^{v+1}J_{v+1}(z)]/\mathrm{d}z = z^{v+1}J_v(z)$ and $\mathrm{d}[z^{-v+1}J_{v-1}(z)]/\mathrm{d}z = -z^{-v+1}J_v(z)$, we can easily calculate the finite Hankel transforms I_1 and I_2. The finite Hankel transforms of arbitrary functions can be obtained by integrating by parts and using the series expansion form of the Bessel functions for small arguments and/or a numerical integration. In this study, the following transforms are needed:

$$I_3(\xi_i) = \int_{r_1}^{r_2} r^2D_v(\xi_i r)\,\mathrm{d}r, \qquad I_4(\xi_i) = \int_{r_1}^{r_2} r^2\ln(r_2/r)D_v(\xi_i r)\,\mathrm{d}r, \tag{58}$$

$$I_5(\xi_i) = \int_{r_1}^{r_2} r^2\ln(r/r_1)D_v(\xi_i r)\,\mathrm{d}r, \qquad I_{6n}(\xi_i) = \int_{r_1}^{r_2} r^2\ln(r\alpha_n/2)D_v(\xi_i r)\,\mathrm{d}r, \tag{59}$$

$$I_{7nk}(\xi_i) = \int_{r_1}^{r_2} r^{2k+4}\ln(r\alpha_n/2)D_v(\xi_i r)\,\mathrm{d}r, \quad I_{8nk}(\xi_i) = \int_{r_1}^{r_2} r^{2k+4}D_v(\xi_i r)\,\mathrm{d}r. \tag{60}$$

For large arguments, in terms of α_n, the finite Hankel transforms are

$$I_{6Lnk}(\xi_i) = \int_{r_1}^{r_2} r(r\alpha_n)^{-2k-1/2}\cos(r\alpha_n/2)D_v(\xi_i r)\,\mathrm{d}r, \tag{61}$$

$$I_{7Lnk}(\xi_i) = \int_{r_1}^{r_2} r(r\alpha_n)^{-2k-1/2}\sin(r\alpha_n/2)D_v(\xi_i r)\,\mathrm{d}r, \tag{62}$$

$$I_{8Lnk}(\xi_i) = \int_{r_1}^{r_2} r(r\alpha_n)^{-2k-3/2}\cos(r\alpha_n/2)D_v(\xi_i r)\,\mathrm{d}r, \tag{63}$$

$$I_{9Lnk}(\xi_i) = \int_{r_1}^{r_2} r(r\alpha_n)^{-2k-3/2}\sin(r\alpha_n/2)D_v(\xi_i r)\,\mathrm{d}r. \tag{64}$$

The numerical integration cannot be avoided for the evaluation of these integral transforms. It can be noted that the numerical Hankel transform is always possible for arbitrary functions.

Combining all expressions, the finite Hankel transform of the dynamic component of the displacement, from Eq. (51), is

$$\widehat{u_{\mathrm{d}}}(\xi_i,t) = -\widehat{U_{\mathrm{o}}}(\xi_i)\cos\bar{c}\xi_i t + \sum_{n=1}^{\infty}\widehat{R}_n(\xi_i)\left[\bar{c}\xi_i I_0(t) - \Omega_n(t)\right], \tag{65}$$

where the convolution integral $I_0(t) = \int_{\mathrm{o}}^{t}\Omega_n(\tau)\sin\bar{c}\xi_i(t-\tau)\mathrm{d}\tau$ and $\Omega_n(t) = \mathrm{e}^{-K\alpha_n{}^2 t}$ as described earlier. Substituting $\widehat{u_{\mathrm{d}}}(\xi_i,t)$ into Eq. (47), the general solution of the dynamic elasticity part of the equation of motion is obtained as

$$U_{\mathrm{d}}(r,t) = \sum_i \frac{D_v(\xi_i r)}{N(\xi_i)}\left\{ -\widehat{U_{\mathrm{o}}}(\xi_i)\cos\bar{c}\xi_i t + \sum_{n=1}^{\infty}\widehat{R}_n(\xi_i)\left[\bar{c}\xi_i I_0(t) - \Omega_n(t)\right]\right\}. \tag{66}$$

Therefore, the general elastodynamic solution for the thermal shock problem of orthotropic thick shells is found to be

$$U(r,t) = U_{\mathrm{o}}(r) + \sum_{n=1}^{\infty}R_n(r)\Omega_n(t) + \sum_i \frac{D_v(\xi_i r)}{N(\xi_i)}\left\{ -\widehat{U_{\mathrm{o}}}(\xi_i)\cos\bar{c}\xi_i t + \sum_{n=1}^{\infty}\widehat{R}_n(\xi_i)\left[\bar{c}\xi_i I_0(t) - \Omega_n(t)\right]\right\}. \tag{67}$$

After obtaining the displacement field, the elastodynamic thermal shock stresses can be determined from the strain–displacement and the orthotropic stress–strain relations. In particular, the radial stress is

$$\sigma_{rr}(r,t) = c_{11}\frac{\partial U(r,t)}{\partial r} + c_{12}\frac{U(r,t)}{r} + c_{13}f(t) - q_1 T(r,t). \tag{68}$$

The circumferential stress is given by

$$\sigma_{\theta\theta}(r,t) = c_{12}\frac{\partial U(r,t)}{\partial r} + c_{22}\frac{U(r,t)}{r} + c_{23}f(t) - q_{\alpha 2}T(r,t), \tag{69}$$

and the axial stress is given by

$$\sigma_{zz}(r,t) = c_{31}\frac{\partial U(r,t)}{\partial r} + c_{32}\frac{U(r,t)}{r} + c_{33}f(t) - q_3 T(r,t), \tag{70}$$

where $q_{\alpha 2} = c_{21}\alpha_r + c_{22}\alpha_\theta + c_{23}\alpha_z$. Using Eqs. (3) and (67), the following expression can be written, in lieu of Eq. (68)

$$\sigma_{rr}(r,t) = G_{10}B_{11} + G_{20}B_{12} + f_{\mathrm{o}}B_{13} + B_{14} + \sum_{n=1}^{\infty}G_{1n}B_{11n} + G_{2n}B_{12n} + f_n B_{13n} + B_{14n}, \tag{71}$$

where B_{ij} and B_{ijn} are provided in Appendix D. Similar expressions can be obtained for $\sigma_{\theta\theta}$ and σ_{zz}.

The unknown constants, can now be determined from the boundary conditions. We assume that no external tractions exist on the boundaries. Then, the conditions on the bounding surfaces (at r_1 and r_2) can be written in the following form:

$$\sigma_{rr}(r_i,t) = \tau_{r\theta}(r_i,t) = \tau_{rz}(r_i,t) = 0, \quad i = 1,2. \tag{72}$$

Only a condition for the stress σ_{rr}, written as Eq. (71), is not satisfied identically. Substituting Eq. (67) into Eq. (72), the following two linear equations in terms of the unknown constants G_{10}, G_{20} and f_0, are obtained:

$$G_{10}(c_{11}\lambda_1 + c_{12})r_i^{\lambda_1-1} + G_{20}(c_{11}\lambda_2 + c_{12})r_i^{\lambda_2-1} + f_0\left[c_{13} + \frac{c_{23}-c_{13}}{c_{11}-c_{22}}(c_{11}+c_{12})\right]$$
$$= -c_{11}U_o^{*\prime}(r_i) - \frac{c_{12}}{r_i}U_o^*(r_i) + q_1[d_1 + d_2\ln(r_2/r_i) + d_3\ln(r_i/r_1)], \quad i = 1,2. \tag{73}$$

Similarly, for the other set of unknown constants G_{1n}, G_{2n} and f_n

$$G_{1n}(c_{11}+c_{12})r_i^{\lambda_1-1} + G_{2n}(c_{11}+c_{12})r_i^{\lambda_2-1} + f_n\left[c_{13} + \frac{c_{23}-c_{13}}{c_{11}-c_{22}}(c_{11}+c_{12})\right]$$
$$= -c_{11}R_n^{*\prime}(r_i) - \frac{c_{12}}{r_i}R_n^*(r_i) + q_1[d_{4n}J_0(r\alpha_n) + d_{5n}Y_0(r\alpha_n)], \quad i = 1,2. \tag{74}$$

The end condition of zero resultant axial force (13) gives the last set of equations that are needed to determine the unknown constants G_{10}, G_{20} and f_0

$$G_{10}\frac{c_{31}\lambda_1 + c_{32}}{\lambda_1+1}(r_2^{\lambda_1+1} - r_1^{\lambda_1+1}) + G_{20}\frac{c_{31}\lambda_2 + c_{32}}{\lambda_2+1}(r_2^{\lambda_2+1} - r_1^{\lambda_2+1}) + f_0\left(\frac{c_{23}^2 - c_{13}^2}{c_{11}-c_{22}} + c_{33}\right)\frac{(r_2^2 - r_1^2)}{2}$$
$$= -c_{31}\left[rU_o^*(r)\right]_{r_1}^{r_2} - (c_{23}-c_{13})\int_{r_1}^{r_2} U_o^*(r_i)\,\mathrm{d}r + q_3\left[(d_1 + d_2/2 - d_3/2)\frac{(r_2^2 - r_1^2)}{2}\right.$$
$$\left. + (d_3 r_2^2 - d_2 r_1^2)\frac{\ln(r_2/r_1)}{2}\right], \tag{75}$$

and similarly for G_{1n}, G_{2n} and f_n,

$$G_{1n}\frac{(c_{31}\lambda_1 + c_{32})}{\lambda_1+1}(r_2^{\lambda_1+1} - r_1^{\lambda_1+1}) + G_{2n}\frac{(c_{31}\lambda_2 + c_{32})}{\lambda_2+1}(r_2^{\lambda_2+1} - r_1^{\lambda_2+1}) + f_n\left[\frac{c_{23}^2 - c_{13}^2}{c_{11}-c_{22}} + c_{33}\right]\frac{(r_2^2 - r_1^2)}{2}$$
$$= -c_{31}\left[rR_n^*(r)\right]_{r_1}^{r_2} - (c_{32}-c_{13})\int_{r_1}^{r_2} R_n^*(r)\,\mathrm{d}r + q_3\left\{\frac{d_{4n}}{\alpha_n}[r_2J_1(r_2\alpha_n) - r_1J_1(r_1\alpha_n)]\right.$$
$$\left. + \frac{d_{5n}}{\alpha_n}[r_2Y_1(r_2\alpha_n) - r_1Y_1(r_1\alpha_n)]\right\}. \tag{76}$$

The time-dependent terms in the boundary conditions (71) as given by the sets of linear algebraic equations (72)–(75) automatically vanish since the boundary conditions (34) and (35) for the dynamic elasticity part are homogeneous.

3. Results and discussion

The thermal shock stresses are obtained from this elastodynamic solution in an orthotropic thick cylindrical shell. The finite Hankel transform and the Laplace transform are used for solving the dynamic part. These integral transformations have been successfully applied to the problem without any inversion difficulties. For the series sum of dynamic solution, the roots of the nonlinear equation (42) are used. Numerical finite Hankel transformations for arbitrary functions are carried out by the Romberg's integration algorithm.

For an illustrative example, the following information is used for a glass/epoxy circular cylinder of inner radius $r_1 = 20$ mm and outer radius $r_2 = 40$ mm, made by filament winding with the fibers oriented around the circumference. The moduli in GN m^{-2} and Poisson's ratios for the material are listed below, where 1 represents the radial (r) direction, 2 the circumferential (θ) direction, and 3 the axial (z) direction

$$E_1 = E_3 = 19.8, \qquad E_2 = 48.3, \qquad G_{12} = G_{23} = 8.96,$$
$$G_{31} = 6.19, \qquad \nu_{12} = \nu_{23} = 0.27, \qquad \nu_{31} = 0.60.$$

The thermal expansion coefficients are $\alpha_r = \alpha_z = 15 \times 10^{-6}\,^{\circ}\mathrm{C}^{-1}$, $\alpha_\theta = 0.23 \times 10^{-6}\,^{\circ}\mathrm{C}^{-1}$. The thermal diffusivity in the radial direction is $K = 0.112 \times 10^{-5}\ \mathrm{m^2\,s^{-1}}$.

Assume that a temperature of $T_o = 300^{\circ}\mathrm{C}$ above the reference is suddenly applied at $r = r_1$, while there is heat convection to the surrounding air at $r = r_2$. It is assumed that the loading temperature T_o causing the thermal shock is maintained thereafter. In this case, the coefficients in Eq. (2) are $h_1 = h_3^* = 0$, $h_1^* = h_2 = 1$, $h_2^* = h$, $h_3 = -T_o$, where h is the ratio of the convective heat-transfer coefficient between the composite tube and the surrounding medium at $r = r_2$ and the thermal conductivity of the tube in the radial direction. A typical value for heat convection to the air is $h = 0.15\ \mathrm{m^{-1}}$.

In order to present the results, the following nondimensional quantities are used $r^* = (r - r_1)/(r_2 - r_1)$ for the radial distance (through the thickness) and $t^* = ct/(r_2 - r_1)$ for the nondimensional time. In the following, the behavior of the elastodynamic thermal shock stresses which propagate through the wall as a stress wave will be described.

In Fig. 1, the wave propagation of radial stress at the center of wall, $r^* = 0.5$, is shown during the early moments after heating. The stress wave is initiated at the inside surface, where the loading is applied, and reflected at the boundary surface after propagating through the wall. The propagation and reflection of the stress wave lead to stress reversions throughout the thickness. The magnitude and direction of stress depends on the location of the wave front. The radial stress is periodically changed from compression to tension or from tension to compression. The stress pattern varies as time passes due to interferences of waves. This effect increases with time. In this figure, it is noted that the tensile radial stress exists until the thermally induced disturbance reaches the location, $r^* = 0.5$, because the region where the temperature has not conducted yet, plays the role of a "rigid band" in the sense that this region has not been disturbed in the first phase yet. Dynamic radial stress always switches from tension to compression at the location $r^* = 0.5$,

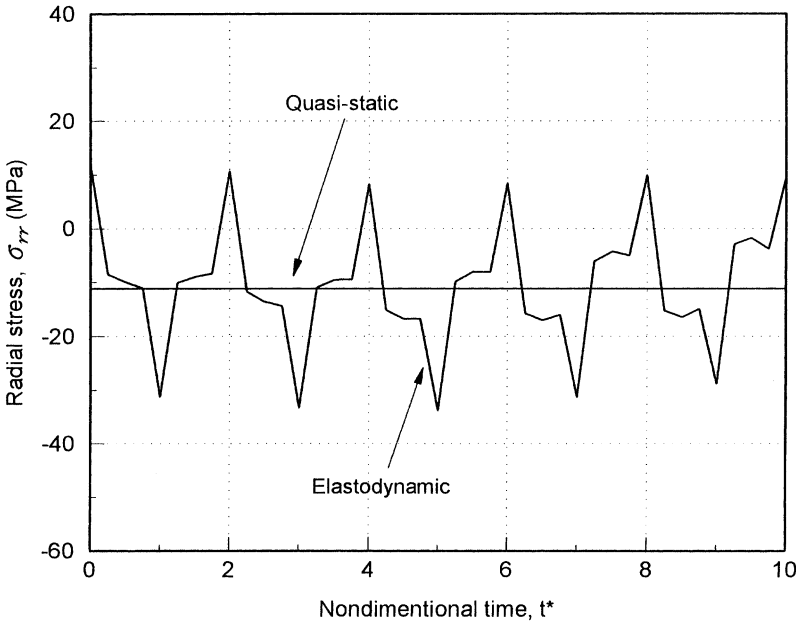

Fig. 1. The propagation of the radial stress wave, $\sigma_{rr}(r,t)$, at $r^* = 0.5$, with the normalized time, which is defined as $t^* = ct/(r_2 - r_1)$.

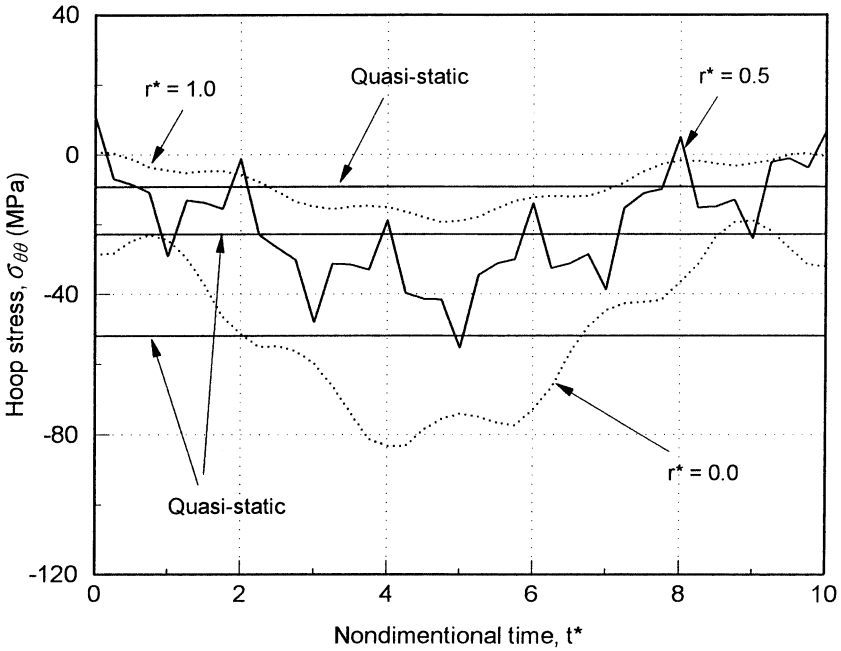

Fig. 2. The variation of the hoop stress, $\sigma_{\theta\theta}(r,t)$, at $r^* = 0, 0.5, 1.0$, with the normalized time, $t^* = ct/(r_2 - r_1)$.

even though the quasi-static radial stress always stays in compression. Fig. 2 shows the tangential (hoop) stress at different locations. The maximum stress is obtained at the inside surface of a hollow cylinder. The hoop stress at $r^* = 0.5$ shows the characteristic stress wave propagation with its periodical variation. This figure shows that the hoop stress at each location stays in compression. This fact is true in the initial phase after the loading since this is applied at the inside surface of a hollow cylinder. The axial stress response in the early phase is presented in Fig. 3. Similar behaviors are shown. The largest axial stress exists at the inside boundary right after the heating.

The above results, as explained earlier, are presented for a realistic inertia parameter γ which is defined as $\gamma = K/c(r_2 - r_1)$ and required a very small stepsize of time, less than 10^{-5} to 10^{-6} for acceptable computing results. Therefore, the above results show more precisely the behavior of thermal shock stress wave propagation and reflection through the wall. The stress discontinuity is well shown in those figures. This time step computation could not be done without high performance computer resources. A detailed discussion about this point is also provided by Tsui and Kraus (1965) and Zaker (1969).

As an alternative validation for the above results, which were presented for a realistic inertia parameter, the following was done. The temperature history in terms of another nondimensionalized time $t' = Kt/(r_2 - r_1)^2$ is given in Fig. 4 at different locations. The corresponding actual time of t^* is much less than that of t'. It is known that temperatures at each location are fully delivered quickly after the loading. The hoop stress response in nondimensional time t' at the locations $r^* = 0, 1$ is shown in Fig. 5. An inertia parameter $\gamma = 1/5$, is used to see inertia effects (Tsui and Kraus, 1965; Zaker, 1969). This inertia parameter is not realistic, but was used in these earlier studies. The dynamic effect as seen in Fig. 1 remains even in this manner. The validity of the results in Fig. 5 is verified by comparison with results from these earlier studies. The thermal shock stress behavior is well shown and it has similar patterns as those in (Sumi and Ito's 1993) study. Fig. 5 shows the thermal shock stress when the inertia parameter is set to $\gamma = 1/5$, which is an unrealistically large value.

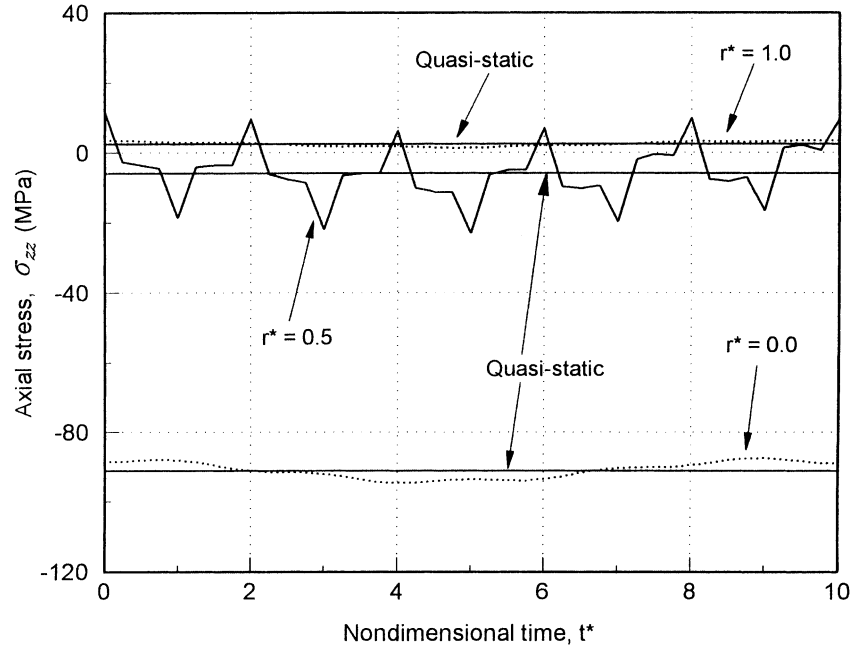

Fig. 3. The variation of the axial stress, $\sigma_{zz}(r,t)$, at $r^* = 0, 0.5, 1.0$, with normalized time, $t^* = ct/(r_2 - r_1)$.

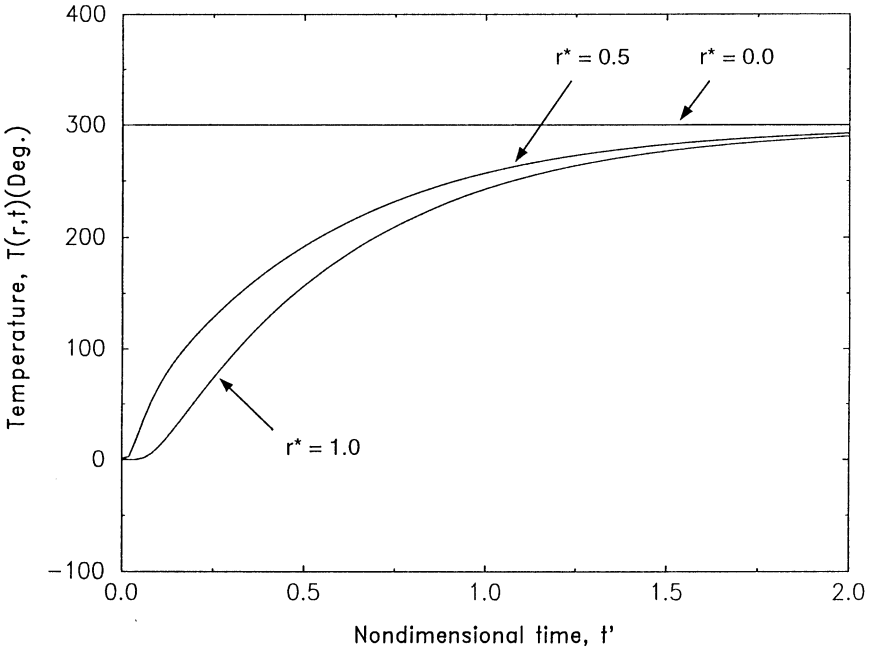

Fig. 4. The temperature history, $T(r,t)$, as a function of the normalized time, $t' = Kt/(r_2 - r_1)^2$, at the locations $r^* = 0, 0.5, 1.0$.

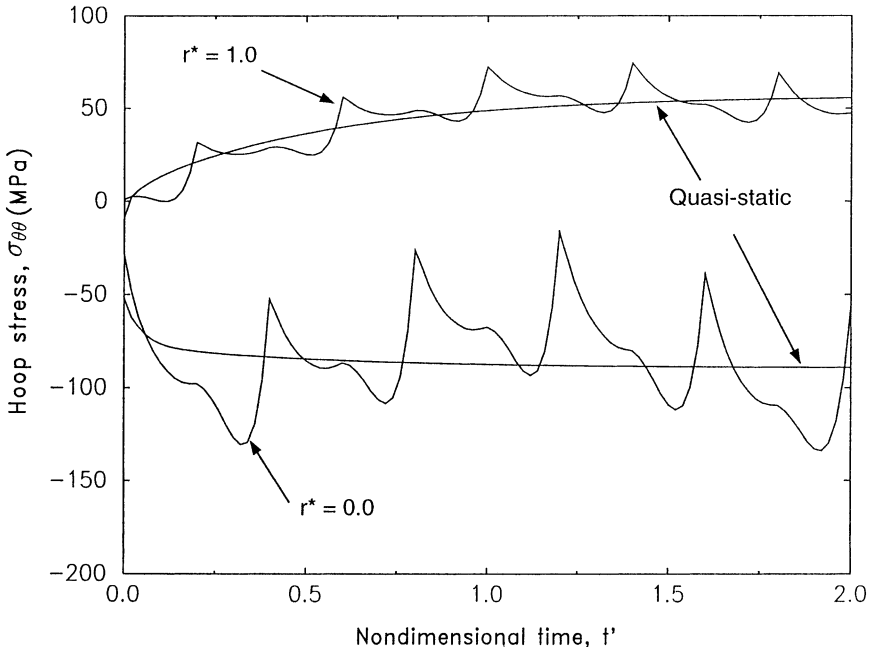

Fig. 5. The hoop stress variation, $\sigma_{\theta\theta}(r,t)$, with normalized time, $t' = Kt/(r_2 - r_1)^2$, at the locations $r^* = 0, 1.0$. A large (unrealistic) inertia parameter $\gamma = K/c(r_2 - r_1) = 1/5$ is used.

In order to complete this study from the early moment after the loading to the time that the temperature reaches to quite a steady state in any location, dynamic stresses are presented in terms of a nondimensional time t' with a realistic inertia parameter. Displacements at different locations are shown in Fig. 6. Displacements are seen to vary uniformly, but their derivatives show some variations as shown in Figs. 6–8. As expected, the points at $r^* = 0$ move inward of the cylinder, while the points at $r^* = 1$ move outward. All these dynamic displacements essentially oscillate around the quasistatic values. The time history of hoop stress at different locations $r^* = 0, 0.5, 1$ is plotted in Fig. 7. The maximum hoop stress is obtained at $r^* = 0$, which is the inside bounding surface. It is always compressive. The quasi-static hoop stress at $r^* = 0.5$ varies from compression to tension. Fig. 8 is for the time history of axial stress at different locations. It is interesting that the axial stress at the inside surface varies from the largest value at the initial stage to a smaller one. Thus, this axial stress should be watched since cylindrical structures made by circumferentially filament wounding would be inherently weak in the axial direction. The significance of stress variation with time is seen in all stress components and is particularly noticeable for the hoop stress at the inner wall of cylinder, $r^* = 0$.

4. Summary

The elastodynamic solution for thermal shock stresses in an orthotropic cylindrical shell due to heat transfer into/from a medium (e.g. fluid) at a constant temperature is obtained. The stress wave propagation phenomenon is clearly shown. It is found that the dynamic contribution combined with the thermal and material orthotropy cannot be neglected on the thermoelastic stress response (variation) when the heating is applied rapidly. In other words, orthotropic properties in addition to inertia effects on disturbance should

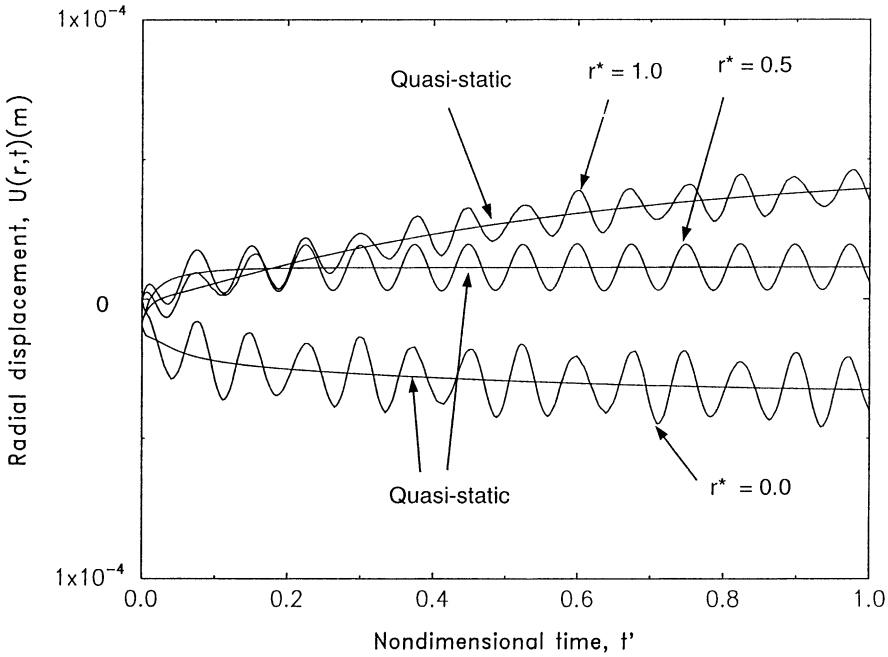

Fig. 6. The time history of the displacements, $U(r,t)$, at $r^* = 0, 0.5, 1.0$ in nondimensional time, t', defined as $t' = Kt/(r_2 - r_1)^2$. A smaller, realistic value of the inertia parameter γ is used.

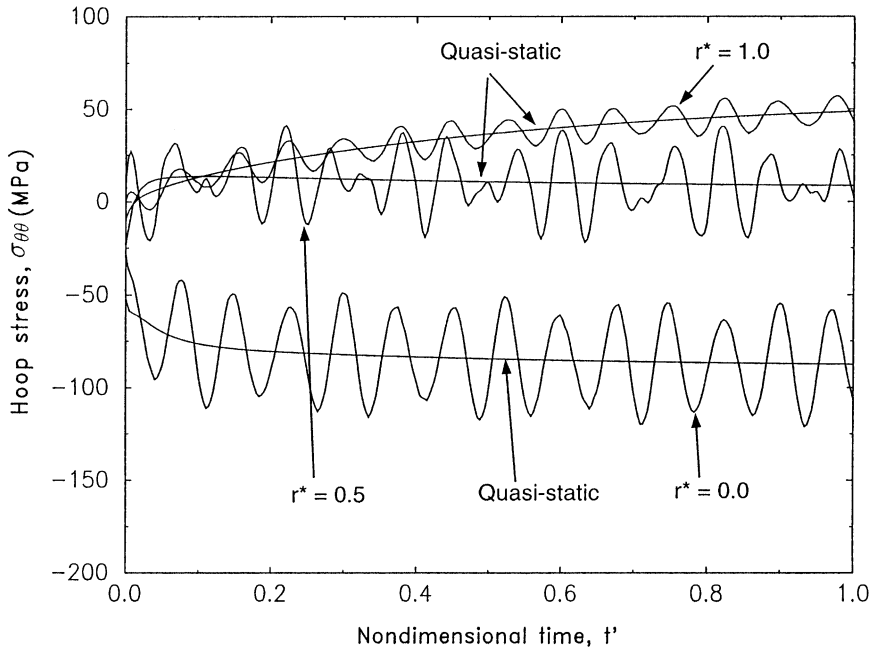

Fig. 7. The time history of the hoop stress, $\sigma_{\theta\theta}(r,t)$, at $r^* = 0, 0.5, 1.0$.

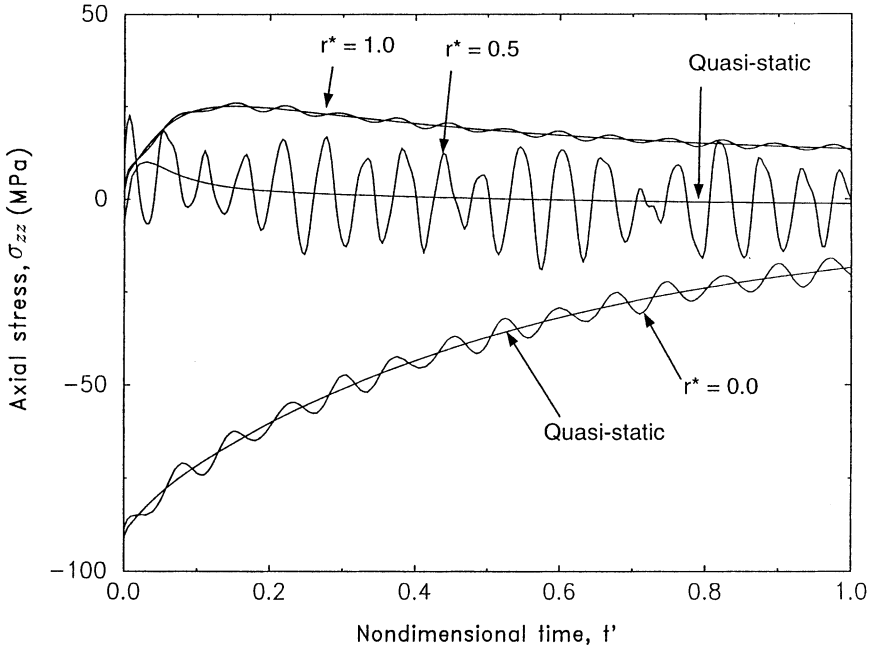

Fig. 8. The time history of the axial stress, $\sigma_{zz}(r,t)$, at $r^* = 0, 0.5, 1.0$.

be considered. Differences between quasi-static and dynamic stresses are clear in all stress components. These dynamic contributions of stresses, which cannot be captured by a static or quasi-static analysis, could play unexpected roles on the structure's integrity. It is noted that a transient thermal stress analysis without the dynamic contribution would arrive at the steady state rapidly even though at these time values the dynamic stress components due to inertia effects would still remain. As is well known, the thermal deformation is largely influenced by the thermal expansion coefficients. Thus, needless to say, the thermal expansion coefficients are very important factors, together with the orthotropic stiffness properties of the material in thermo-elastic stress analyses.

Acknowledgements

The financial support of the Office of Naval Research, Ship Structures and Systems, S&T Division, Grant N00014-91-J-1892, and the interest and encouragement of the Grant Monitor, Dr. Y.D.S. Rajapakse, are both gratefully acknowledged.

Appendix A

In the temperature distribution $T(r,t)$ in Eq. (3), the coefficients d_1, d_2 and d_3 used are expressed in terms of

$$\Delta = r_1 h_2 h_1^* + r_2 h_1 h_2^* + r_1 r_2 h_2 h_2^* \ln(r_2/r_1), \tag{A.1}$$

as

$$d_1 = \frac{r_2 h_1 h_3^* - r_2 h_3 h_1^*}{\Delta}, \quad d_2 = \frac{r_1 r_2 h_3 h_2^*}{\Delta}, \quad d_3 = -\frac{r_1 r_2 h_2 h_3^*}{\Delta}. \tag{A.2}$$

The constants d_{4n} and d_{5n} are given in terms of

$$F_1(\alpha_n) = \left[h_1^* \alpha_n J_1(r_2\alpha_n) - h_2^* J_0(r_2\alpha_n)\right] \times \left\{h_3\left[h_1^* \alpha_n J_1(r_2\alpha_n) - h_2^* J_0(r_2\alpha_n)\right] - h_3^*\left[h_1 \alpha_n J_1(r_1\alpha_n) + h_2 J_0(r_1\alpha_n)\right]\right\}^2, \tag{A.3}$$

$$F_2(\alpha_n) = (h_1^{*^2}\alpha_n^2 + h_2^{*^2})\left[h_1 \alpha_n J_1(r_1\alpha_n) + h_2^* J_0(r_1\alpha_n)\right]^2 - (h_1^2\alpha_n^2 + h_2^2)\left[h_1^* \alpha_n J_1(r_2\alpha_n) - h_2^* J_0(r_2\alpha_n)\right]^2, \tag{A.4}$$

as follows:

$$d_{4n} = -\pi \frac{F_1(\alpha_n)}{F_2(\alpha_n)}\left[h_1 \alpha_n Y_1(r_1\alpha_n) + h_2 Y_0(r_1\alpha_n)\right], \tag{A.5}$$

$$d_{5n} = \pi \frac{F_1(\alpha_n)}{F_2(\alpha_n)}\left[h_1 \alpha_n J_1(r_1\alpha_n) + h_2 J_0(r_1\alpha_n)\right]. \tag{A.6}$$

It should be noted that the case of $h_2 = h_1^* = 0$ is excluded.

Appendix B

The solution $R_n(r)$ in Eq. (22) has the coefficients

$$B_{1nk} = \frac{2d_{5n}(-1)^{k+1}\alpha_n^{2k+2}[q_2 + 2q_1(k+1)]}{\pi 2^{2k+2}[(k+1)!]^2[c_{11}(2k+3)^2 - c_{22}]}, \tag{B.1}$$

$$B_{2nk} = \frac{(-1)^{k+1}\alpha_n^{2k+2}}{2^{2k+2}[(k+1)!]^2[c_{11}(2k+3)^2 - c_{22}]} f_{kn} - \frac{B_{1nk} 2c_{11}(2k+3)}{[c_{11}(2k+3)^2 - c_{22}]}, \tag{B.2}$$

where

$$f_{kn} = \left[d_{4n} - \frac{2d_{5n}}{\pi}\left(1 + \frac{1}{2} + \cdots + \frac{1}{k+1} - \gamma_o\right)\right][q_2 + 2q_1(k+1)] + \frac{2d_{5n}q_1}{\pi}, \tag{B.3}$$

where γ_o is the Euler constant.

Appendix C

The series expansion form of the Bessel functions is defined as follows:

$$J_v(x) = \sum_{m=0}^{\infty} A_m x^{2m+v}, \qquad J_{-v}(x) = \sum_{n=0}^{\infty} A_{-m} x^{2m-v}, \tag{C.1}$$

where

$$A_m = \frac{(-1)^m (1/2)^{2m+v}}{m!\Gamma(m+v+1)}, \qquad A_{-m} = \frac{(-1)^m (1/2)^{2m-v}}{m!\Gamma(m-v+1)}.$$

The Hankel asymptotic expansions of the Bessel functions for large arguments are, when v is fixed and $|z|$ tends to infinity, described as

$$J_v(z) = \sqrt{2/(\pi z)}[P(v,z)\cos\chi - Q(v,z)\sin\chi], \tag{C.2}$$

$$Y_v(z) = \sqrt{2/(\pi z)}[P(v,z)\sin\chi + Q(v,z)\cos\chi], \tag{C.3}$$

where $\chi = z - (\frac{1}{2}v + \frac{1}{4})\pi$ and, with $4v^2$ denoted by μ,

$$P(v,z) = \sum_{k=0}^{\infty}(-1)^k \frac{(v,2k)}{(2z)^{2k}} = 1 - \frac{(\mu-1)(\mu-9)}{2!(8z)^2} + \cdots \tag{C.4}$$

$$Q(v,z) = \sum_{k=0}^{\infty}(-1)^k \frac{(v,2k+1)}{(2z)^{2k+1}} = \frac{(\mu-1)}{(8z)} - \frac{(\mu-1)(\mu-9)(\mu-25)}{3!(8z)^3} + \cdots \tag{C.5}$$

Appendix D

In the expression for the radial dynamic stress given by Eq. (71), the coefficients are

$$B_{11} = (c_{11}\lambda_1 + c_{12})r_i^{\lambda_1-1} + \sum_i \left[c_{11}\frac{\mathrm{d}D_v(\xi_i r_i)}{\mathrm{d}r} + \frac{c_{12}}{r_i}D_v(\xi_i r)\right] I_1(\xi_i)V_o(\xi_i,t), \tag{D.1}$$

$$B_{12} = (c_{11}\lambda_2 + c_{12})r_i^{\lambda_2-1} + \sum_i \left[c_{11}\frac{\mathrm{d}D_v(\xi_i r_i)}{\mathrm{d}r} + \frac{c_{12}}{r_i}D_v(\xi_i r)\right] I_1(\xi_i)V_o(\xi_i,t), \tag{D.2}$$

$$B_{13} = c_{13} + \frac{c_{23}-c_{13}}{c_{11}-c_{22}}(c_{11}+c_{12}) + \frac{c_{23}-c_{13}}{c_{11}-c_{22}}\sum_i \left[c_{11}\frac{\mathrm{d}D_v(\xi_i r_i)}{\mathrm{d}r} + \frac{c_{12}}{r_i}D_v(\xi_i r)\right] I_1(\xi_i)V_o(\xi_i,t), \tag{D.3}$$

$$\begin{aligned} B_{14} = {} & -c_{11}U_o^{*'}(r_i) - \frac{c_{22}}{r}U_o^*(r_i) + q_{\alpha 1}[d_1 + d_2\ln(r_2/r_i) + d_3\ln(r_i/r_1)] \\ & - \sum_i \left[c_{11}\frac{\mathrm{d}D_v(\xi_i r_i)}{\mathrm{d}r} + \frac{c_{12}}{r_i}D_v(\xi_i r)\right]\widehat{U}_o^*(r)V_o(\xi_i,t), \end{aligned} \tag{D.4}$$

and

$$B_{11n} = (c_{11}+c_{12})r_i^{\lambda_1-1} + \sum_i \left[c_{11}\frac{\mathrm{d}D_v(\xi_i r_i)}{\mathrm{d}r} + \frac{c_{12}}{r_i}D_v(\xi_i r)\right] I_1(\xi_i)V_n(\xi_i,t)\Omega_n^{-1}(t), \tag{D.5}$$

$$B_{12n} = (c_{11}+c_{12})r_i^{\lambda_2-1} + \sum_i \left[c_{11}\frac{\mathrm{d}D_v(\xi_i r_i)}{\mathrm{d}r} + \frac{c_{12}}{r_i}D_v(\xi_i r)\right] I_1(\xi_i)V_n(\xi_i,t)\Omega_n^{-1}(t), \tag{D.6}$$

$$B_{13n} = c_{13} + \frac{c_{23}-c_{13}}{c_{11}-c_{22}}(c_{11}+c_{12}) + \frac{c_{23}-c_{13}}{c_{11}-c_{22}}\sum_i \left[c_{11}\frac{\mathrm{d}D_v(\xi_i r_i)}{\mathrm{d}r} + \frac{c_{12}}{r_i}D_v(\xi_i r)\right] I_1(\xi_i)V_n(\xi_i,t)\Omega_n^{-1}(t), \tag{D.7}$$

$$\begin{aligned} B_{14n} = {} & -c_{11}R_n^{*'}(r_i) - \frac{c_{22}}{r}R_n^*(r_i) + q_{\alpha 1}[d_{4n}J_0(r\alpha_n) + d_{5n}Y_0(r\alpha_n)] \\ & - \sum_i \left[c_{11}\frac{\mathrm{d}D_v(\xi_i r_i)}{\mathrm{d}r} + \frac{c_{12}}{r_i}D_v(\xi_i r)\right] H[R_n^*(r)]V_n(\xi_i,t)\Omega_n^{-1}(t), \end{aligned} \tag{D.8}$$

where the inverse of $\Omega_n(t)$ can be written as $\Omega_n^{-1}(t) = \mathrm{e}^{K\alpha_n^2 t}$ and the time-dependent terms are described by

$$V_o(\xi_i,t)=\frac{(\bar{c}\xi_i\sin\bar{c}\xi_i t-1)}{N(\xi_i)},\qquad V_n(\xi_i,t)=\frac{\bar{c}\xi_i I_0(t)-\Omega_n(t)}{N(\xi_i)}. \tag{D.9}$$

Similarly, the definitions for B_i and B_{in} of the other expressions can be evaluated if c_{11}, c_{12} and c_{13} are replaced by c_{21}, c_{22} and c_{23} and by c_{31}, c_{32} and c_{33}.

References

Carslaw, H.S., Jaeger, S.C., 1959. Conduction of Heat in Solids, second ed. Clarendon Press, Oxford.

Cho, H., Kardomateas, G.A., Valle, C.S., 1998. Elastodynamic solution for the thermal shock stresses in an orthotropic thick cylindrical shell. Journal of Applied Mechanics ASME 65 (1), 184–193.

Cinelli, G., 1965. An extension of the finite Hankel transform and applications. International Journal of Engineering Science 3, 539–559.

Hata, T., 1991. Thermal shock in a hollow sphere caused by rapid uniform heating. Journal of Applied Mechanics ASME 58, 64–69.

Hyer, M.W., Cooper, D.E., 1986. Stresses and deformations in composite tubes due to a circumferential temperature gradient. Journal of Applied Mechanics ASME 53, 757–764.

Kardomateas, G.A., 1989. Transient thermal stresses in cylindrical orthotropic composite tubes. Journal of Applied Mechanics ASME 56, 411–417.

Kardomateas, G.A., 1990. The initial phase of transient thermal stresses due to general boundary thermal stresses due to general thermal loads in orthotropic hollow cylinders. Journal of Applied Mechanics ASME 57, 719–724.

Lekhnitskii, S.G., 1981. Theory of Elasticity of an Anisotropic Body. Mir Publishers, Moscow.

Sternberg, E., Chakravorty, J.G., 1959. Thermal shock in an elastic body with a spherical cavity. Quarterly of Applied Mathematics 17, 205–218.

Sumi, N., Ito, Y., 1993. The propagation and reflection of thermal stress waves in anisotropic nonhomogeneous hollow cylinders and spheres. Nuclear Engineering and Design 140, 133–145.

Tsui, T., Kraus, H., 1965. Thermal stress wave propagation in hollow elastic spheres. Journal of the Acoustical Society of America 37, 730–737.

Wang, X., 1995. Thermal shock in a hollow cylinder caused by rapid arbitrary heating. Journal of Sound and Vibration 183 (5), 899–906.

Yuan, F.G., 1993. Thermal stresses in thick laminated composite shells. Composite Structures 26, 63–75.

Zaker, T.A., 1969. Dynamic thermal shock in a hollow sphere. Quarterly of Applied Mathematics 26, 503–520.